Pairing Symmetry and Upward Curvature of Upper Critical Field in Superconducting $Na_{0.35}CoO_2 \cdot yH_2O$

Jun-Ting Kao,[1] Jiunn-Yuan Lin,[2] and Chung-Yu Mou[1,3]

[1] *Department of Physics, National Tsing Hua University, Hsinchu 30043, Taiwan*
[2] *Institue of Physics, National Chao Tung University, Hsinchu 30043, Taiwan*
[3] *Physics Division, National Center for Theoretical Sciences, P.O.Box 2-131, Hsinchu, Taiwan*

(Dated: February 6, 2008)

The origin for the upward curvature of the upper critical field (H_{c2}) observed in hydrate cobaltate $Na_{0.35}CoO_2 \cdot yH_2O$ is investigated based on the microscopic gap equation. It is shown that the observed upward curvature results from the transition between two different pairing symmetries that occur on different energy bands. Furthermore, different pairing symmetries involved in the transition results in different upward curvatures. By considering transitions among all lowest possible pairing symmetries, it is found that the transition of the pairing symmetry from s-wave at low fields to $d_{x^2-y^2} + id_{xy}$ at high fields is the best fit to the experimental data. Our results provide an important clue to the understanding of the superconductivity in hydrate cobaltate.

PACS numbers: 73.20.-r, 73.20.At, 73.21.Hb

Since the discovery of superconductivity in hydrate cobaltate $Na_{0.35}CoO_2 \cdot yH_2O$[1], extensive theoretical and experimental studies have been devoted to elucidate the mechanism of superconductivity. To unravel the mechanism, identifying the underlying pairing symmetry would be the first step. The two-dimensional triangle lattice formed by CoO_2 provides an alternative lattice symmetry to the square CuO_2 lattice in high Tc materials and has led to many proposals for unconventional pairing symmetries. For singlet pairing, the lowest possible unconventional symmetry without breaking rotational symmetry is $d_{x^2-y^2} \pm id_{xy}$, and mechanism based on the correlation effects for such symmetry has been proposed[2, 3, 4]. Possible spin-triplet f-wave pairing was also proposed based on ferromagnetic fluctuations[5, 6, 7]. Experimentally, however, data reported show contradictory conclusions[8], indicating the fragility of the superconductivity in this system. Furthermore, there are evidences indicating that two pairing symmetries may be involved in this system [9, 10, 11]. The issue of whether the pairing symmetry is conventional or not is still unsettled and needs to be clarified.

In this paper, we shall focus on the data of the upper critical fields, measured by the specific heat. The specific-heat technique probes the bulk properties of the samples and has been proved to be a powerful tool for investigating the pairing state of many superconductors[12]. Specifically, for the hydrate cobaltate $Na_{0.35}CoO_2 \cdot yH_2O$, upward curvature (a kink structure in the slope) of H_{c2} was observed [9, 10]. Similar structure was also observed in early studies of high Tc materials[13]. Based on the Ginzburg-Landau theory, Joynt[14] attributed the upward curvature to the transition between two different pairing symmetries with different critical temperatures. However, in a later investigation based on microscopic formulation of the gap equation [15], negative results were found, indicating that the upward curvature is not due to mixing of two pairing order parameters. The reason why two approaches give different results lies in the fact that in the Ginzburg-Landau theory, $H_{c2} \propto T - T_c$ and phenomenologically, both T_c and slopes of H_{c2} are often chosen arbitrarily. If larger slope of H_{c2} is chosen for smaller T_c, H_{c2} of two pairing symmetries near their T_c's essentially shows the intersection of two straight lines. A kink in the slope thus arises and the upward curvature can be easily simulated. In real materials, however, the slope of H_{c2} and T_c both depend on microscopic details and are not independent from each other. In fact, in the Gorkov's microscopic derivation of the Ginzburg-Landau equation[16], the slope is proportional to m^*T_c/ϵ_F with m^* being the effective mass of the electron and ϵ_F being the Fermi energy. For a single band, m^*/ϵ_F are the same for different pairing symmetries, hence smaller T_c goes with smaller slope, in the opposite trend adopted in the Ginzburg-Landau equation. Hence in this case, joining two pairing symmetries with different T_c would not yield the upward curvature. This picture essentially explains why the upward curvature is not reproduced in the calculation of Kim et al. [15] for high Tc materials. Then, what is the origin for the upward curvature in hydrate colaltate ? It is known that multi-orbitals near the Fermi surface might be involved for the occurrence of superconductivity[17]. Hence m^*/ϵ_F can no longer be treated as a fixed parameter for different pairing symmetries if different pairings occur on different bands. Indeed, our calculation in below shows that upward curvature feature can result from the two-band calculation in which different values of m^*/ϵ_F are assumed for different energy bands where different pairing symmetry occurs. Furthermore, mixing of different pairing symmetries results in coupling of the ground state to different Landau levels in the presence of magnetic fields and causes different upward curvatures. By direct comparison of experimental data with H_{c2} obtained by mixing of the lowest

possible pairing symmetries, it is possible to pin down the pairing symmetries of the system. We find that the upward curvature observed in the experimental data is mostly consistent with a transition of the pairing symmetry from s to $d_{x^2-y^2}+id_{xy}$.

We start by first considering pairing that occurs in two bands. The two-dimensional BCS-like Hamiltonian can be written as

$$\hat{H} = \sum_{i=1}^{2}\sum_{k_i,\sigma}\xi_{k_i}\hat{C}^{+}_{k_i\sigma}\hat{C}_{k_i\sigma} + \sum_{i,j}\sum_{k_i,k'_j} V_{k_ik'_j}\hat{C}^{+}_{k_i\uparrow}\hat{C}^{+}_{-k_i\downarrow}\hat{C}_{-k'_j\downarrow}\hat{C}_{k'_j\uparrow}, \quad (1)$$

which was first investigated by Suhl, Matthias, and Walker[18]. Here $\mathbf{k}_1$ and $\mathbf{k}_2$ are wave vectors on two Fermi surface sheets indexed by 1 and 2. The electron-electron interaction $V_{\mathbf{k}_1\mathbf{k}'_1}$ and $V_{\mathbf{k}_2\mathbf{k}'_2}$ are the intrasheet contributions and $V_{\mathbf{k}_1\mathbf{k}'_2}$ is an intersheet contribution. In general, the superconducting pairing symmetry is different for different band. Hence we can write the projection of the interaction in the form $V_{\mathbf{k}_1\mathbf{k}'_1} = V_\alpha\hat{\phi}_\alpha(\mathbf{k}_1)\hat{\phi}^*_\alpha(\mathbf{k}'_1)$, $V_{\mathbf{k}_2\mathbf{k}'_2} = V_\beta\hat{\phi}_\beta(\mathbf{k}_2)\hat{\phi}^*_\beta(\mathbf{k}'_2)$, and $V_{\mathbf{k}_1\mathbf{k}'_2} = V_I\hat{\phi}_\alpha(\mathbf{k}_1)\hat{\phi}^*_\beta(\mathbf{k}'_2)$. Here α and β are indices for the pairing symmetry. $\hat{\phi}_\alpha(\mathbf{k})$ is an operator that projects out the corresponding pairing symmetry α. For the lowest possible pairings, we shall consider possible mixing of p and f waves for triplet pairing and mixing of s and d for singlet pairing. For the triangle lattice, assuming that the rotational symmetry is not broken, the appropriate p and d pairing amplitudes are $p_x \pm ip_y$ and $d_{x^2-y^2} \pm id_{xy}$. The corresponding projection operators are $\hat{\phi}_s(\mathbf{k}) = 1$, $\hat{\phi}_{p\pm ip}(\mathbf{k}) = \hat{k}_x \pm i\hat{k}_y$, $\hat{\phi}_{d\pm id}(\mathbf{k}) = \hat{k}^2_x - \hat{k}^2_y \pm 2i\hat{k}_x\hat{k}_y$, and $\hat{\phi}_f(\mathbf{k}) = \hat{k}^3_x - 3\hat{k}_x\hat{k}^2_y$. Note that there are two possible f-waves; however, since they are related by a rotation of $\pi/6$ and it suffices to consider one of them (see below for details). Following Kim et al.[15], the real-space linearized gap equation in the presence of the magnetic field $\nabla\times\mathbf{A}$ can be written as[15]

$$\Delta_\alpha(\mathbf{R}) = V_\alpha\sum_\omega\int d\mathbf{r}\hat{\phi}^*_\alpha(\phi)\hat{\phi}_\alpha(\phi)\hat{K}_1(\mathbf{r},\omega)\Delta_\alpha(\mathbf{R}) + V_I\sum_\omega\int d\mathbf{r}\hat{\phi}^*_\alpha(\phi)\hat{\phi}_\beta(\phi)\hat{K}_2(\mathbf{r},\omega)\Delta_\beta(\mathbf{R}), \quad (2)$$

and

$$\Delta_\beta(\mathbf{R}) = V_\beta\sum_\omega\int d\mathbf{r}\hat{\phi}^*_\beta(\phi)\hat{\phi}_\beta(\phi)\hat{K}_2(\mathbf{r},\omega)\Delta_\beta(\mathbf{R}) + V_I\sum_\omega\int d\mathbf{r}\hat{\phi}^*_\beta(\phi)\hat{\phi}_\alpha(\phi)\hat{K}_1(\mathbf{r},\omega)\Delta_\alpha(\mathbf{R}). \quad (3)$$

Here $\mathbf{R}$ represents the position for the center of mass of the Cooper pair, $\mathbf{r}$ is the displacement of the Cooper pair and ϕ is the corresponding angle of $\mathbf{r}$. Δ's are pairing amplitudes in real space and $\hat{\phi}_\alpha(\phi)$ are the projection operators in real space: $\phi_s(\phi) = 1$, $\phi_{p\pm ip}(\phi) = e^{\pm i\phi}$, $\phi_{d\pm id}(\phi) = e^{\pm 2i\phi}$, and $\phi_f(\phi) = \cos^3\phi - 3\cos\phi\sin^2\phi = cos3\phi$. $\hat{K}_i(\mathbf{r},\omega)$ is the kernel operator, given by

$$\hat{K}_i(\mathbf{r},\omega) = K^0_i(\mathbf{r},\omega)\exp\left[\mathbf{r}\cdot(\bigtriangledown_{\mathbf{R}} + \frac{2ie}{\hbar c}\mathbf{A}(\mathbf{R}))\right] \quad (4)$$

with

$$K^0_i(\mathbf{r},\omega) = k_BTN_i(0)^2\frac{2\pi}{k_{Fi}}\frac{\exp\left[\frac{-2r|\omega|}{v_{Fi}}\right]}{r}, \quad (5)$$

where k_{Fi}, v_{Fi} and $N_i(0)$ are the Fermi wavenumber, Fermi velocity and the two dimensional density of state for the ith band. In the absence of V_I, Eqs.(2) and (3) decouples, and their solutions for constant Δ and $\mathbf{A} = 0$ yield relations between T_c and V_α[19]

$$\frac{1}{\Gamma_iV_iN_i} = \sum_\nu\frac{1}{|2\nu+1|} - \ln\frac{T^i_c}{T}, \quad (6)$$

where $i = \alpha$ or β with T^i_c being the corresponding transition temperature in zero field and $\Gamma_i = \int^{2\pi}_0\frac{d\phi}{2\pi}|\hat{\phi}_i(\phi)|^2$. Dividing Eqs.(2) and (3) by V_α and V_β respectively and using Eq.(6), V_α and V_β can be eliminated. Following Ref.[19], if we further adopt dimensionless variables, $\mathrm{t_i} = \mathrm{T/T^i_c}$, $\mathbf{r} = \rho/\sqrt{2eH/\hbar c}$ and $h_i = 2eH/\hbar c(\hbar v_{Fi}/2\pi k_BT^i_c)^2$, the gap equations become

$$\Gamma_\alpha\left(\sum_\nu\frac{1}{|2\nu+1|} - \ln\frac{1}{t_\alpha}\right)\Delta_\alpha(\mathbf{R}) = \hat{K}_{\alpha\alpha}\Delta_\alpha(\mathbf{R}) - \xi_\alpha\gamma\hat{K}_{\alpha\beta}\Delta_\beta(\mathbf{R}) \quad (7)$$

$$\Gamma_\beta\left(\sum_\nu\frac{1}{|2\nu+1|} - \ln\frac{1}{t_\beta}\right)\Delta_\beta(\mathbf{R}) = \hat{K}_{\beta\beta}\Delta_\beta(\mathbf{R}) - \frac{\xi_\beta}{\gamma}\hat{K}_{\beta\alpha}\Delta_\alpha(\mathbf{R}), \quad (8)$$

where $\xi_i = V_I/V_i$ and $\gamma = N_\beta/N_\alpha$. The operators $\hat{K}$ are given by

$$\hat{K}_{nm} = \frac{1}{2\pi}\frac{t_m}{\sqrt{h_m}}\sum_\omega\int^\infty_0 d\rho\ \exp\left[\frac{-\rho}{\alpha^m_\omega}\right]\ \exp\left[\frac{-\rho^2}{4}\right] \times\int^{2\pi}_0 d\phi\hat{\phi}^*_n(\phi)\hat{\phi}_m(\phi)\exp\left[\frac{-\rho}{\sqrt{2}}\hat{a}^+e^{i\phi}\right]\exp\left[\frac{\rho}{\sqrt{2}}\hat{a}^-e^{-i\phi}\right], \quad (9)$$

where $\alpha^m_\omega = \frac{\sqrt{\frac{2eH}{\hbar c}}}{2|\omega|}v_{Fm}$ and $\hat{a}^\pm = \sqrt{\frac{\hbar c}{4eH}}[(\bigtriangledown + 2ieA)_x \pm i(\bigtriangledown + 2ieA)_y]$.

Eqs.(7) and (8) are the governing equations for the situation when two pairing symmetries occur on different energy bands. However, it also covers the case when the two pairing symmetries occur in the same energy band. In that case, one simply sets $\gamma = 1$, $\xi_i = 1$, and drop the

index i. Eqs.(7) and (8) can be solved by expanding Δ_α and Δ_β in terms of the set of eigenfunctions $|\psi_n\rangle$ of the two-dimensional Schrodinger equation in the presence of $\mathbf{A} = (0, Hx, 0)$

$$\Delta_i = \sum_{n=0}^{\infty} A_n^i |\psi_n\rangle, \tag{10}$$

where $i = \alpha$ or $i = \beta$. Note that the eigenfunctions $|\psi_n\rangle$ are essentially the Landau levels. The operators $\hat{K}$ couple different Landau levels. The detailed coupling is determined by the bi-product projection operator, $\hat{\phi}_n^*(\phi)\hat{\phi}_m(\phi)$, in Eq.(9), which, after being integrated, selects the correct combinations of $\hat{a}^+$ and $\hat{a}^-$ that survive. The selected combination of $\hat{a}^+$ and $\hat{a}^-$ then determines how A_n^i couple. For the mixing of s-wave and $d + id$, $\{A_n^s\}$ couples with $\{A_{n+2}^{d+id}\}$; while for the mixing of s-wave and $d - id$, $\{A_n^s\}$ couples with $\{A_{n-2}^{d+id}\}$. On the other hand, for the mixing of $p \pm ip$ and f-wave, because $\hat{\phi}_f(\phi)$ contains both $e^{3i\phi}$ and $e^{-3i\phi}$, in addition to the coupling between $A_n^{p\pm ip}$ and A_n^f, there are also couplings among $\{A_n^f\}$. Since the bi-product projection operator in $\hat{K}_{ff}$, $\hat{\phi}_f^*(\phi)\hat{\phi}_f(\phi)$, contains $e^{\pm i6\phi}$, A_n^f couples with A_{n+6}^f for each n; while because the bi-product projection operators in off-diagonal $\hat{K}_{\alpha\beta}$ ($\alpha \neq \beta$), contains $e^{\pm i4\phi}$ and $e^{\pm i2\phi}$, we found that $\{A_n^f\}$ couple with $\{A_{n+4}^{p+ip}\}$ and $\{A_n^f\}$ couple with $\{A_{n+2}^{p-ip}\}$. The coupling coefficients are most conveniently expressed in terms of the following functions[15]

$$\beta_n^i = \frac{t_i}{\sqrt{h_i}} \int_0^\infty d\rho \ \frac{e^{-\frac{\rho^2}{4}} L_n\left(\frac{\rho^2}{2}\right) - 1}{\sinh\left(\frac{t_i\rho}{\sqrt{h_i}}\right)} \tag{11}$$

and

$$\alpha^i(2k, n) = \frac{t_i}{\sqrt{h_i}} \int_0^\infty d\rho \ \frac{e^{\frac{-\rho^2}{4}} \left(\frac{-\rho^2}{2}\right)^k L_n^{2k}\left(\frac{\rho^2}{2}\right)}{\sinh\left(\frac{t_i\rho}{\sqrt{h_i}}\right)}, \tag{12}$$

where i is the index for the pairing symmetry, $L_n(x)$ is the Laguerre polynomial and L_n^{2k} is the associated Laguerre polynomial in Rodrigues representation. For triplet pairing, we find that recursion relations for the mixing of f-wave with $p_x \pm ip_y$ are given by

$$\begin{aligned}
&\frac{-1}{2}\sqrt{\frac{(n-6)!}{n!}}\alpha^f(6, n-6)A_{n-6}^f + \left(\ln\frac{1}{t_f} + \beta_n^f\right)A_n^f \\
&-\frac{1}{2}\sqrt{\frac{(n+6)!}{n!}}\alpha^f(-6, n+6)A_{n+6}^f \\
&+\xi_f\gamma\sqrt{\frac{(n\mp 2)!}{n!}}\alpha^{p\pm ip}(\pm 2, n\mp 2)A_{n\mp 2}^{p\pm ip} \\
&-\xi_f\gamma\sqrt{\frac{(n\pm 4)!}{n!}}\alpha^{p\pm ip}(\mp 4, n\pm 4)A_{n\pm 4}^{p\pm ip} = 0,
\end{aligned} \tag{13}$$

and

$$\begin{aligned}
&\left(\ln\frac{1}{t_p} + \beta_n^p\right)A_n^{p\pm ip} - \frac{\xi_{p\pm ip}}{2\gamma}\sqrt{\frac{(n\mp 4)!}{n!}}\alpha^f(\pm 4, n\mp 4)A_{n\mp 4}^{1f} \\
&+\frac{\xi_{p\pm ip}}{2\gamma}\sqrt{\frac{(n\pm 2)!}{n!}}\alpha^f(\mp 2, n\pm 2)A_{n\pm 2}^f = 0.
\end{aligned} \tag{14}$$

On the other hand, for singlet pairing, recursion relations for the mixing of s-wave with $d_{x^2-y^2} \pm id_{xy}$ are given by

$$\left(\ln\frac{1}{t_s} + \beta_n^s\right)A_n^s + \frac{\xi_s}{\gamma}\sqrt{\frac{(n\pm 2)!}{n!}}\alpha^{d\pm id}(\mp 2, n\pm 2)A_{n\pm 2}^{d\pm id} = 0, \tag{15}$$

and

$$\left(\ln\frac{1}{t_d} + \beta_n^d\right)A_n^{d\pm id} + \xi_{d\pm id}\gamma\sqrt{\frac{(N\mp 2)!}{n!}}\alpha^s(\pm 2, n\mp 2)A_{n\mp 2}^s = 0. \tag{16}$$

When applying the above analysis to the calculation of H_{c2} with mixing of two pairing symmetries, α and β, one assumes that the pairing symmetries are associtaed with different T_c's with $T_c^\alpha > T_c^\beta$. In other word, the pairing symmetry α is the stable bulk pairing state at low fields while β is the stable pairing state at high fields. Therefore, one starts from $\Delta_\alpha = A_0^\alpha|\psi_0\rangle$. Mixing to the other symmetry, β, then couples A_0^α to A_n^β with $n \geq 1$. Since $\{A_n^s\}$ couples with $\{A_{n\pm 2}^{d\pm id}\}$, this analysis implies that one can only have the transitions from high-temperature s-wave to low-temperature $d + id$ or from high-temperature $d - id$ to low-temperature s-wave. On the other hand, for the mixing of $p \pm ip$ and f-wave, because $\hat{\phi}_f(\phi)$ contains both $e^{3i\phi}$ and $e^{-3i\phi}$, both transitions from high-temperature $p \pm ip$ to low-temperature f-wave and from high-temperature f-wave to low-temperature $p \pm ip$ are possible. Note that there are two possible f-waves, $\hat{k}_x^3 - 3\hat{k}_x\hat{k}_y^2$ and $\hat{k}_y^3 - 3\hat{k}_y\hat{k}_x^2$. Since the two f-waves are related by exchanging $\hat{k}_x$ and $\hat{k}_y$ which simply exchanges p_x+ip_y and p_x-ip_y, it suffices to consider one of them.

When solving H_{c2}, it is important to note that there are many eigenvalues $H(T)$ satisfying Eqs.(7) and (8) and only the largest one defines H_{c2}. To compare the calculated H_{c2} with experimental data, one needs to fix scales of temperatures and magnetic fields. The transition temperature T_c of the most stable bulk pairing state determines the temperature scale. On the other hand, the scale of magnetic fields can be fixed by the data points with lower magnetic fields. The remaining parameters are the ratio of Fermi velocities, the ratio of T_c, ξ_i and γ. At this point, it is important to note that according to Eqs. (13)-(16), for different mixing scheme, different Landau levels are mixed. As a result, different mixing scheme results in different upward curvature. To find the best fit to the experimental data, after fixing scales of temperatures and magnetic fields, we vary

the remaining parameters to find the best. We find that the transition from s-wave at low fields to $d+id$ at high fields is the best fit to the data. In Fig. 1, we show numerical results of H_{c2} for the transition from s-wave at low fields to $d+id$ at high fields in comparison with experimental data obtained by specific-heat measurement. The fitting parameters are the ratio of Fermi velocities $v_F^s/v_F^{d+id} = 0.8$, $T_c^{d+id}/T_c^s = 0.5$, $\xi_s = 4.3$, $\xi_{d+id} = 0.89$, and $\gamma = 1.1$. These values are in reasonable regime. The close fitting ro the experimental data clearly shows that singlet pairing dominates in hydrate cobaltat, which is also consistent with recent NMR data[20]. Furthermore, it implies that two energy bands are involved and supports results based on LDA calculations[17] where two bands constructed from the three Co t_{2d} orbitals intersect the Fermi level.

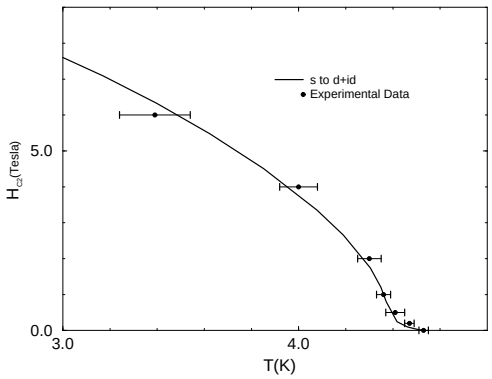

FIG. 1: The comparison of experimental data of H_{c2}[9] with numerical results based on the transition from s-wave at low fields to $d+id$ at high fields.

In conclusion, we have investigated the origin for the upward curvature of the upper critical field (H_{c2}) observed in hydrate cobaltate $Na_{0.35}CoO_2 \cdot yH_2O$. Analysis based on the microscopic gap equation shows that the observed upward curvature results from the transition between two different pairing symmetries that occur on different energy bands. Furthermore, it is found that the transition of the pairing symmetry from s-wave at low fields to $d_{x^2-y^2} + id_{xy}$ at high fields is the best fit to the experimental data.

This work is supported by the NSC of Taiwan. We thank Prof. Hsiu-Hau Lin for useful discussions.

[1] K. Takada, H. Sakurai, E. Takayama-Muromachi, F. Izumi, R. A. Dilanian, and T. Sasaki, Nature **422**, 53, (2003).

[2] G. Baskaran, Phys. Rev. Lett. **91** 097003 (2003).

[3] Q.H. Wang, D.-H. Lee, and P.A. Lee, Phys. Rev. B **69**, 092504 (2004).

[4] M. Ogata, J. Phys. Soc. Jpn. **72**, 1839 (2003).

[5] A.Tanaka and X. Hu, Phys. Rev. Lett. **91**, 257006 (2003).

[6] K. Kuroki, Y. Tanaka, and R. Arita, Phys. Rev. Lett. **93**, 077001 (2004).

[7] M. Mochizuki, Y. Yanase, and M. Ogata , Phys. Rev. Lett. **94**, 147005 (2005).

[8] See I. I. Mazin and M. D. Johannes, Nature Physics **1**, 91-93 (2005) and reference therein.

[9] H. D. Yang, J.-Y. Lin, C. P. Sun, Y. C. Kang, C. L. Huang, K. Takada, T. Sasaki, H. Sakurai, and E. Takayama-Muromachi, Phys. Rev. B **71**, 020504(R) (2005).

[10] M. M. Maska, M. Mierzejewski, B. Andrzejewski, M. L. Foo, R. J. Cava, and T. Klimczuk, Phys. Rev. B **70**, 144516 (2004).

[11] Masahito Mochizuki and Masao Ogata, cond-mat/0610562.

[12] See, for example, K. A. Moler, D. L. Sisson, J. S. Urbach, M. R. Beasley, A. Kapitulnik, D. J. Baar, R. Liang, and W. N. Hardy, Phys. Rev. B **55**, 3954 (1997); D. A. Wright, J. P. Emerson, B. F. Woodfield, J. E. Gordon, R. A. Fisher, and N. E. Phillips, Phys. Rev. Lett. **82**, 1550 (1999); and H. D. Yang, J.-Y. Lin, H. H. Li, F. H. Hsu, C. J. Liu, S.-C. Li, R.-C. Yu, and C.-Q. Jin, Phys. Rev. Lett. **87**, 167003 (2001).

[13] T. K. Worthington, W. J. Gallagher, and T. R. Dinger, Phys. Rev. Lett. **59**, 1160 (1987).

[14] R. Joynt, Phys. Rev. B **41**, 4271(1990).

[15] Wonkee Kim, Jian-Xin Zhu, and C. S. Ting, Phys. Rev. B **58**, R607(1998).

[16] A. Fetter and J. D. Walecka, *Quantum Theory of Many-Particle Systems*, Ch. 13 (McGraw-Hill, San Francisco, 1971).

[17] D. J. Singh, Phys. Rev. B **61**, 13397(2000); M. D. Johannes and D. J. Singh, Phys. Rev. B **70**, 014507 (2004); K.-W. Lee, J. Kunes, and W. E. Pickett, Phys. Rev. B **70**, 045104 (2004).

[18] H. Suhl, B. T. Matthias, and L. R. Walker, Phys. Rev. Lett. **3**, 552 (1959).

[19] E. Helfand and N. R. Werthamer, Phys. Rev. Lett. **13**, 686 (1964); Phys. Rev. **147**, 288 (1966)

[20] Y. Kobayashi, M. Yokoi and M. Sato, J. Phys. Soc. Jpn. **72**, 2126 (2003); Y. Kobayashi, H. Watanabe, M. Yokoi, T. Moyoshi, Y. Mori and M. Sato, J. Phys. Soc. Jpn. **74**, 1800 (2005).